Design and Clinical Validation of a Robotic Ankle-Foot Simulator With Series Elastic Actuator for Ankle Clonus Assessment Training

Yinan Pei, Tianyi Han, Christopher M. Zallek, Tao Liu, Liangjing Yang, and Elizabeth T. Hsiao-Wecksler

***Abstract*—To fulfill the need for reliable and consistent medical training of the neurological examination technique to assess ankle clonus, a series elastic actuator (SEA) based haptic training simulator was proposed and developed. The simulator's mechanism (a hybrid of belt and linkage drive) and controller (impedance control) were designed to render a realistic and safe training environment. Benchtop tests demonstrated that the prototype simulator was able to accurately estimate the interaction torque from the trainee (average RMSE of 0.2 Nm) and closely track a chirp torque command up to 10 Hz (average RMSE of $<$0.22 Nm). The high-level impedance controller could switch between different clinically encountered states (i.e., no clonus, unsustained clonus, and sustained clonus) based on trainee's assessment technique. The simulator was evaluated by a group of 17 experienced physicians and physical therapists. Subjects were instructed to induce sustained clonus using their normal technique. The simulator was assessed in two common clinical positions (seated and supine). Subjects scored simulation realism on a variety of control features. To expedite controller design iteration, feedback from Day 1 was used to modify simulation parameters prior to testing on Day 2 with a new subject group. On average, all subjects could successfully trigger a sustained clonus response within 4-5 attempts in the first position and 2-3 in the second. Feedback on the fidelity of simulation realism improved between Day 1 and Day 2. Results suggest that this SEA-based simulator could be a viable training tool for healthcare trainees learning to assess ankle clonus.**

***Index Terms*—Medical robots and systems, haptics and haptic interfaces, education robotics, human-centered robotics, physical human-robot interaction.**

Manuscript received October 15, 2020; accepted February 24, 2021. Date of publication March 11, 2021; date of current version March 30, 2021. This letter was recommended for publication by Associate Editor L. Masia and Editor P. Valdastri upon evaluation of the reviewers' comments. This work was supported by the University of Illinois at Urbana Champaign and Zhejiang University Joint Research Funding Program. *(Corresponding author: Yinan Pei.)*

Yinan Pei and Elizabeth T. Hsiao-Wecksler are with the Department of Mechanical Science and Engineering, University of Illinois at Urbana-Champaign, Urbana, IL 61801 USA (e-mail: pei2@illinois.edu; ethw@illinois.edu).

Tianyi Han and Liangjing Yang are with the Zhejiang University International Campus, Haining, China (e-mail: tianyih4@illinois.edu; liangjingyang@intl.zju.edu.cn).

Christopher M. Zallek is with the Department of Neurology, OSF HealthCare Illinois Neurological Institute, Peoria, IL 61603 USA (e-mail: christopher.m.zallek@ini.org).

Tao Liu is with the School of Mechanical Engineering, Zhejiang University, Hangzhou 310027, China (e-mail: liutao@zju.edu.cn).

This letter has supplementary downloadable material available at https://doi.org/10.1109/LRA.2021.3065242, provided by the authors.

Digital Object Identifier 10.1109/LRA.2021.3065242

I. Introduction

A. Significance of Medical Robotic Training

During neurological examinations, clinicians need to perform manual assessment techniques (e.g., passive stretching of affected muscles, tapping the tendon) to elicit clinical signs to diagnose neurological conditions and rely on haptic experiential knowledge to evaluate muscle tone. Although more advanced non-invasive assessment techniques are emerging [1], [2], manual physical assessment is still standard in the clinical setting. Therefore, it is imperative to afford new clinicians, residents, and students more exposure to the haptic feeling of common abnormal behaviors during training and to practice their ability to trigger clinical manifestations of neurological conditions and distinguish the severity of the condition [3]–[6]. Traditional clinical training of motor skill assessment is carried out on live subjects. Instructors usually bring in a small number of practice patients into the classroom or let students pretend to be the patient for each other, which leads to limited practice opportunities and inconsistent training outcomes [7]. This training challenge calls for more accessible and consistent ways to provide training opportunities for students that replace or reduce the need for human practice patients [8]. One promising approach is the deployment of medical training simulators.

Although training simulators have been widely adopted in current medical education of surgery, anatomy, and procedures such as IV insertion [8], the training of clinical assessment techniques has received less attention from academia and industry (such that only a few designs have been proposed in the past [7], [9]–[15]). Simulators for clinical assessment training usually take the form of human-sized artificial robotic limbs (lower extremity [14] or upper extremity [7]) with an actuated haptic joint (active [9], [10] or passive [13]) that mimic a patient's joint affected by pathological muscle behaviors due to underlying neurological conditions. The simulated behaviors were created by the modeling of the neurological diseases based on clinical data [9], expert tuning [7], or a combination of them [14]. Such training simulators render a relatively realistic, consistent, and scalable training environment for students, allowing learners to gain hands-on experience without the presence of human patients. Wide-spread implementation of simulators could improve consistency and standardization across different institutions and different methods of teaching, and improve diagnostic and treatment procedures to promote patient healthcare [16]. However, to the authors' knowledge, currently none of previous research prototype simulators were commercialized nor adopted by medical training institutions beyond those authors' home institutions, possibly due to device complexity, maintenance,

This work is licensed under a Creative Commons Attribution 4.0 License. For more information, see https://creativecommons.org/licenses/by/4.0/

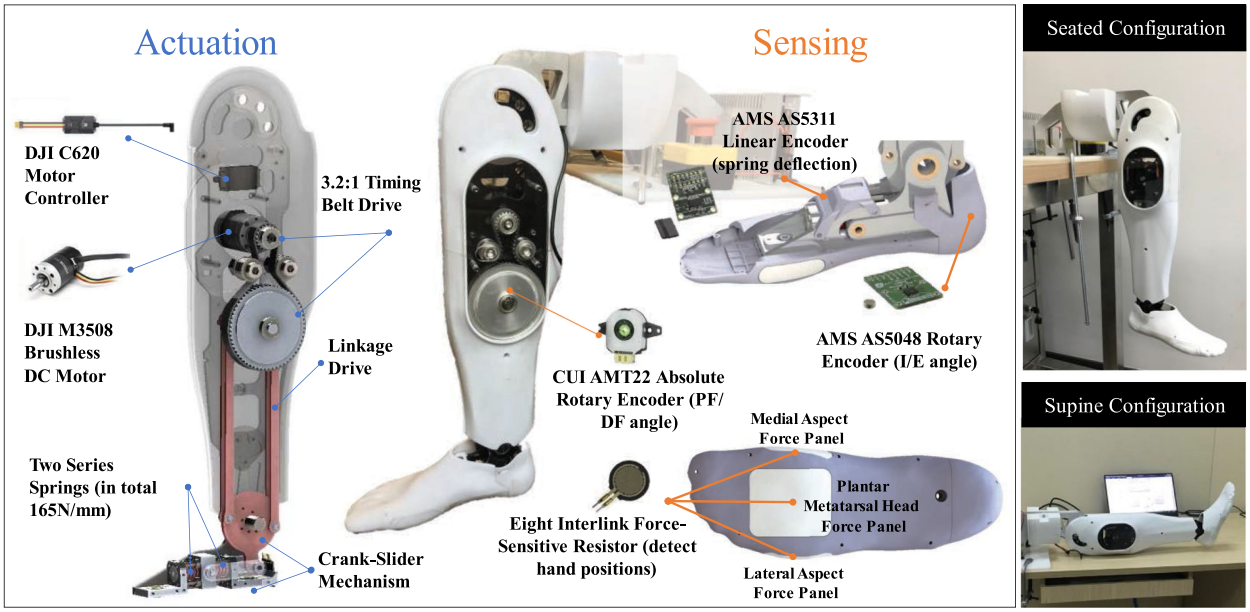

Fig. 1. The ankle-foot training simulator with major actuation and sensing components highlighted, as well as two operation configurations.

or cost. Therefore, we aimed to develop a high-performance, cost-effective, and safe training simulator that is educationally useful and economically viable to be integrated into the curriculum of the training institutions. In the scope of this work, we focused on developing a simulator to help train healthcare learners to perform ankle clonus assessment, a common task during neurological examinations (Fig. 1).

B. Ankle Clonus

Clonus is defined as involuntary and rhythmic muscle contractions caused by lesions in the upper motor neuron pathways [17]–[21]. Although clonus has been reported in muscle groups at other joints, it is most commonly tested and observed at the ankle joint [22]. Ankle clonus can be elicited during a neurological examination by rapidly dorsiflexing (DF) the ankle and maintaining a stretched state of the ankle plantarflexor muscles, as a result of sudden peripheral inputs activating the hyperactive stretch reflex [17], [23]–[26]. Ankle clonus response is a rhythmic oscillation (or "beating") of the foot against an external load with a characteristic frequency between 5–8 Hz [17], [27].

A patient is diagnosed with ankle clonus if the clinician is able to induce a "sustained clonus" response, i.e., five or more consecutive beats. Successful triggering of ankle clonus requires mastery of the following technique [28]: (a) correct positioning of the examining hand on the foot (i.e., evenly supporting on the plantar metatarsal area or grasping both lateral and medial aspects of the forefoot); (b) minimize ankle inversion (i.e., the foot should be in neutral or eversion); (c) provide a rapid dorsiflexion to trigger a stretch reflex (>200 °/s); and (d) maintain constant applied torque on the dorsal surface of the forefoot (>3 Nm). Current medical textbooks often only presented qualitative descriptions of this technique with the absence of numerical values, so the numbers in the parentheses were extracted by the authors from the few available clonus quantification studies or previous attempts on simulating ankle clonus [14], [15], [23], [29], [30]. These numerical values were iterated based on clinical advice (Table I).

TABLE I
A SUMMARY OF PRE-PROGRAMMED CLONUS PARAMETERS. ORIGINAL COLUMN REPRESENTS NUMERICAL DESIGN VALUES INITIALLY EXTRACTED FROM THE LITERATURE. MODIFIED COLUMN LISTS THE REVISED DESIGN VALUESBASED ON 9 EXPERIENCED CLINICIANS ON DAY 1 OF CLINICAL STUDY

	Original	*Modified*
Triggering factors *		
Dorsiflexion speed threshold	> 200° /s	> 150° /s
Hand position panel engagement	Must touch plantar metatarsal head, or both medial and lateral	
Inversion/eversion angle range	> 0°	NA
Sustaining factor		
Sustaining torque threshold	> 3 Nm	> 2 Nm
Clonus Simulation Characteristics *		
Frequency of ankle oscillation	5 Hz	6 Hz
Mean position of ankle oscillation	10° PF	0°
Peak-peak oscillation amplitude	8°	4° (decaying)
Duration	6 s	10 s

*In our convention, dorsiflexion and inversion are negative. Zero angular position is defined at the neutral position (shank perpendicular to foot).

C. State of the Art in Training Simulators for Ankle Clonus

As far as the authors were aware, only two devices exist that attempted to recreate ankle clonus for clinicians to train [14], [15], and no commercially available product exists yet. Kikuchi et al. developed an electromechanical leg-shaped device that used a DC direct-drive motor to generate oscillatory ankle motion to mimic clonus behavior [14]. The motor output torque was transmitted to the user through a magnetorheological fluid (MRF) clutch. The device would switch to the clonus state based on the user's input stretch speed and sustained interaction torque. However, there were a few drawbacks for this design. It lacked a

physiologically-accurate foot shape and the inversion/eversion degree of freedom (DOF) at ankle joint. The device was also mechanically complex due to the use of the MRF clutch. The clutch also introduced unwanted viscous friction torque and as a result the control algorithm had to compute real-time compensation and the device could not command a torque smaller than the viscous torque. Another novel exoskeleton device that created clonus-like behavior on healthy individuals was prototyped by Okumura et al. via a geared DC motor and cable-driven mechanism [15]. The device worn by healthy subjects converted them to mock patients by imposing external actuation force on the wearer's ankle joint to simulate the clonus beats for learners to feel and train. However, several limitations were evident in this design. The force output was relatively small, i.e., 10-20N. Furthermore, the force control performance was not reported, so it was unclear if the device operated in open-loop current control or used a force sensor for closed-loop feedback. The clinical realism of these two devices were either not established [15], or only examined by two clinicians with minimal result reporting [14].

D. Series Elastic Actuators

Although series elastic actuators (SEAs) have been widely used in the robotics community, e.g., humanoids [31], quadruped robots [32], or prosthetics [33], their use has been absent in the field of medical training simulators. Previous robotic simulator designs for motor skill assessment adopted other actuation strategies, such as direct drive [14], quasi-direct drive [9], MRF [7], [14], or electromechanical brake [10]. Direct and quasi-direct drives provided transparent force control capability, but their high operation current and heat dissipation could compromise user safety in human-robot interaction, and the low gear ratio resulted in bulky and nonergonomic joint designs. An MRF brake/clutch was a promising option to generate fast and smooth haptic feeling comparable to human muscle response, but it had to be used in parallel with active actuators to mimic active symptoms (e.g., clonus, tremor, cogwheel rigidity). In addition, off-the-shelf MRF products are not easily available and their sizes are often too bulky for medical applications. Moreover, to generate accurate haptic force, these previous approaches required an external torque sensor to perform closed-loop torque control, which greatly raises device cost.

On the other hand, by deploying a SEA module in our simulator, a relatively high gear ratio would allow a compact motor with reasonable operation current to be used, and a series spring would serve as a compliant and cost-effective torque sensor that could accurately measure interaction joint torque between the user and robot. The intentional introduction of an elastic element will reduce the system control bandwidth and this reduction is usually considered a downside of using a SEA. However, given the low-bandwidth requirement of our application (i.e., 3-8 Hz), this inherent drawback of SEAs would not be a limitation. Thus, these characteristics make a SEA strategy particularly suitable and practical for developing a training simulator with high-fidelity torque control while being cost-effective.

E. Project Overview

In this letter, we present the design and evaluation of a novel ankle clonus training simulator. Haptic feedback force was generated from a series elastic actuator design. The foot-ankle assembly had two degrees of freedom (dorsiflexion-plantarflexion and inversion-eversion) and a realistic foot shroud. Evaluation tests involved benchtop performance experiments and a clinician validation study with experienced physicians and physical therapists.

II. Methods

A. Design Specifications

Our goal was to design a torque-controlled haptic device that rendered a realistic feeling of the muscle response of a patient with ankle clonus to trainees. Considering that an analytical torque-angle profile of ankle clonus is lacking from the literature, the simulated ankle clonus behavior was defined empirically. Specifically, we quantified the ankle clonus assessment into (i) triggering factors, (ii) sustaining factors, and (iii) clonus simulation characteristic parameters (Table I). This quantification of clonus was used to program the simulator's high-level controller, which calculated the simulated clonus muscle tone based on the user's input kinematics. The low-level torque controller was designed to accurately execute the torque command from the high-level controller. In addition, this device should also provide a safe and low-noise training environment for medical instruction.

B. Mechatronic Design and Modeling

The simulator has the appearance of a robotic lower leg, and its segment lengths and 3D-printed shroud contour were designed based on the anthropometric data of a 50^{th} percentile Caucasian male [34] (Fig. 1). To improve device portability (total weight $<$7kg) and reduce rotational inertia of the foot, most structural components were made of FR4 epoxy fiberglass for its high strength-to-weight ratio and the structural design was optimized via topology optimization for balanced stress distribution. The principal DOF was actuated (i.e., dorsiflexion-plantarflexion range of motion (DF/PF ROM): $\pm 30°$). The auxiliary DOF was passive (inversion-eversion (I/E ROM): $\pm 10°$), which was simulated by rotating the foot shroud relative to the underlying structural frame via a pair of inline spherical bearings in the fore and rear foot. The foot shroud geometry and dimensions were obtained from a 3D scanned prosthetic foot (US men's size 10) and the foot's inertial properties were matched with the real human foot [34]. The knee joint can be adjusted and locked easily into a seated or supine position (two common clinical examination poses) with a dowel pin.

The series elastic actuation strategy was chosen for its safe human-robot interaction, accurate force control, robustness, and relatively low cost (Fig. 1) [35]. The specifications of the simulator were derived from previous devices [14], [15]. The actuation torque was exerted via a crank-slider mechanism based on a spring cage mounted in the foot frame (Fig. 1 and 2). The slider in the middle of the spring cage rode on four miniature linear rails with ball bearings. To ensure resistance during both dorsi- and plantarflexion, the slider was preloaded by a die spring (1804N193, McMaster, USA) on each side of the slider, which resulted in a total series spring stiffness of $\sim$165 N/mm. The simulator's drivetrain was actuated by a 150W brushless DC motor with an integrated two-stage planetary gearbox ($\sim$19:1) (M3508, DJI, China), followed by a single-stage 3.2:1 timing belt drive (MR5, Misumi, Japan) and a 1:1 linkage drive. The belt drive was advantageous in quiet and multi-turn operation but if spanning over long distance, its intrinsic compliance will

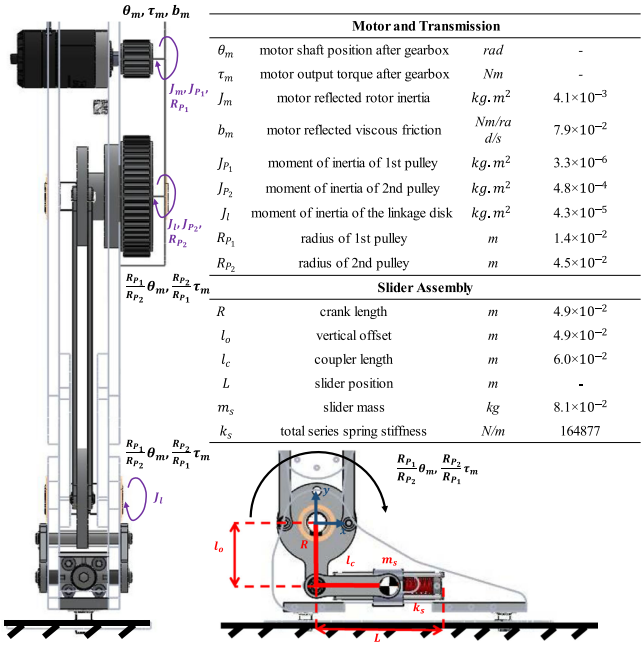

Motor and Transmission			
θ_m	motor shaft position after gearbox	rad	-
τ_m	motor output torque after gearbox	Nm	-
J_m	motor reflected rotor inertia	$kg.m^2$	4.1×10^{-3}
b_m	motor reflected viscous friction	$Nm/rad/s$	7.9×10^{-2}
J_{P_1}	moment of inertia of 1st pulley	$kg.m^2$	3.3×10^{-6}
J_{P_2}	moment of inertia of 2nd pulley	$kg.m^2$	4.8×10^{-4}
J_l	moment of inertia of the linkage disk	$kg.m^2$	4.3×10^{-5}
R_{P_1}	radius of 1st pulley	m	1.4×10^{-2}
R_{P_2}	radius of 2nd pulley	m	4.5×10^{-2}
Slider Assembly			
R	crank length	m	4.9×10^{-2}
l_o	vertical offset	m	4.9×10^{-2}
l_c	coupler length	m	6.0×10^{-2}
L	slider position	m	-
m_s	slider mass	kg	8.1×10^{-2}
k_s	total series spring stiffness	N/m	164877

Fig. 2. Diagram of key parameters in the kinematic and dynamic model.

drop to the similar magnitude of the series springs and influence the effective system stiffness. Therefore, a custom linkage drive consisting of four thin fiberglass bars was combined with the belt drive to transmit actuation torque to the distal ankle joint, keeping the belt span distance minimal. As a result, this drivetrain could generate a peak ankle torque of 17 Nm, with an effective stiffness of ∼5020 N/mm (an order of magnitude larger than the series spring stiffness, thus regarded as rigid).

A dynamic model of the simulator's SEA system was developed to guide choice of series spring stiffness to achieve a torque control bandwidth that was sufficiently high to replicate clonus behavior (Fig. 2 and (1)). The crank-slider mechanism used in this design had nonlinear kinematics. However, given the crank rotation angle would be within only ±2° during operation, the equation of motion was safely linearized around an equilibrium point of crank angle at 0°. In addition, considering that the reflected motor inertia dominated the system's inertia, the model assumed the output end (i.e., simulator's foot) to be fixed on the ground and only the DOF of motor-driven slider movement in the spring cage was modeled to investigate system's natural frequency. Thus, with these two simplifications, the system dynamics were reduced to a 1-DOF linear oscillator (1). For a SEA, the large torque control bandwidth is limited by the open-loop system bandwidth, approximated by the system's fundamental natural frequency. Using (1), the spring stiffness was selected such that the system had a fundamental natural frequency at ∼16 Hz, allowing a torque control bandwidth up to ∼2 times of the maximum clonus motion frequency). This safety factor in control bandwidth was designed to account for any unmodeled dynamics (e.g., bearing friction, spring intrinsic damping, belt compliance) that might slow down the system.

$$0.0041\ddot{\theta}_m + 0.079\dot{\theta}_m + 41\,\theta_m = \tau_{\mathrm{m}} \tag{1}$$

Furthermore, an array of onboard sensing capabilities monitored trainee's performance and provided real-time feedback

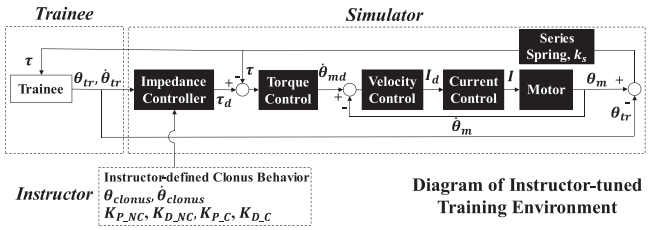

Fig. 3. Simulator's control system diagram with inputs from involved parties (trainee, simulator, and instructor). Subscript d means desired signal.

(Fig. 1). Specifically, a linear encoder (AS5311, ams AG, Austria) mounted on the spring cage to measure spring deflection allowed calculation of the interaction force between the trainee and simulator, as part of the SEA strategy (without the need for expensive load cells). Two DOFs (DF/PF and I/E) of the simulator were sensed by two absolute rotary encoders (AMT22, CUI, USA; and AS5048, ams AG, Austria, respectively). These readings were used in the control logic to define whether the clonus would be triggered based on the trainee's input motion (Table I). Eight force-sensitive resistors (FSRs) (Model 400 and Model 402, Interlink Electronics, USA) were integrated into the foot shroud around the metatarsal heads (plantar, medial and lateral aspects) as simple touch sensors to detect whether the trainee's hand was properly positioned on the forefoot (Table I) [36]. With proper visualization means (e.g., a tablet or screen), data from this sensor array could also provide real-time performance feedback to the trainees for technique correction without the presence of an instructor.

C. Control Strategy

The control system design of the simulator followed the classical control scheme for SEA-based robots (Fig. 3) [37]. The low-level controller had a cascaded architecture (from innermost to outermost: current, velocity, and torque controls) and all loops updated at 1 kHz. The innermost control loop provided proportional-integral (PI) current feedback control and was regulated and executed by a motor controller (C620, DJI, China) with a pre-programmed current loop bandwidth of ∼500Hz. Motor inertia compensation and current command were also implemented as feedforward current inputs. The middle PI velocity loop was added to provide a tight feedback loop around the motor to address backlash in the integrated gearbox. The velocity loop was tuned to achieve a bandwidth of ∼50Hz, roughly 5 times faster than the desired outer torque loop (∼10Hz) to guarantee the separation between servo control loops. Eventually, a proportional-derivative (PD) torque controller (essentially a position controller that modulated the spring deflection, given the SEA architecture) was implemented in the outermost loop that received torque output commands from the high-level controller.

The high-level controller was in the form of an impedance controller that produced a desired torque command (τ_d) and switched between clonus (2) and non-clonus (3) modes by evaluating if all clonus triggering criteria were satisfied (Table I). Each mode was programmed via a desired reference motion trajectory and a set of impedance parameters (2). The estimated torque (τ) was calculated using the known series spring stiffness, crank position (using small-angle approximation), and spring

deflection (ΔL) directly measured by the linear encoder (4).

$$\tau_d = K_{P\_C}(\theta_{clonus} - \theta_{tr}) + K_{D\_C}(\dot{\theta}_{clonus} - \dot{\theta}_{tr}) \quad (2)$$

$$\tau_d = -K_{P\_NC}\theta_{tr} - K_{D\_NC}\dot{\theta}_{tr} \quad (3)$$

$$\tau = k_s R^2 \left(\frac{R_{P_1}}{R_{P_2}}\theta_m - \theta_{tr}\right) = k_s R\Delta L \quad (4)$$

Where θ_{clonus} and $\dot{\theta}_{clonus}$ are reference clonus oscillation ankle angle and angular velocity, while θ_{tr} and $\dot{\theta}_{tr}$ are trainee's input kinematics derived from the DF/PF rotary encoder. In clonus mode, the controller generated a sinusoidal reference angle trajectory with parameters defined in Table I, and the reference velocity was obtained by numerically differentiating the angle trajectory. In the non-clonus mode, the reference angle and angular velocity are 0, meaning that the equilibrium point was at neutral position and zero velocity. The impedance controller was a natural choice to control the ankle motion in the non-clonus mode, i.e., mimicking simplified ankle joint dynamics parametrized by linear stiffness (K_{P_NC}) and damping (K_{D_NC}). The use of an impedance controller also naturally extended to the clonus mode by defining an intensified interaction (due to hyperactive stretch reflex) between rhythmic clonus ankle motion and the trainee's input effort. The K_{P_C} (1 Nm/°) and K_{D_C} (0.03 Nm/(°/s)) were the set of virtual stiffness and damping for the clonus mode; similarly, K_{P_NC} (0.15 Nm/°) and K_{D_NC} (0.01 Nm/(°/s)) for the non-clonus mode. These two sets of impedance parameters were obtained from [29], [30] with slight increase in the damping ratio to improve stability.

All sensors readings were accessed and packed by a lower-level microcontroller (Teeny 3.5, PJRC, USA) and then transmitted to the upper-level microcontroller (TI C2000, TMS28379D, Texas Instrument, USA) at 1.5 kHz. The control system was implemented on the upper-level microcontroller and programmed using Simulink Embedded Coder (MATLAB 2019b, MathWorks, USA).

D. Benchtop Evaluation

A series of benchtop experiments were conducted to evaluate the torque estimation capability of our SEA system, as well as the performance of the low- and high-level controllers. To examine the accuracy of the torque estimated by the SEA system, the motion of the simulator foot was constrained and a torque sensor (TQM301-45N, Omega Engineering Inc., USA) was attached to the ankle joint so that the output torque generated by the motor was measured by the torque sensor. Randomized loadings were exerted on the system by manually rotating the motor rotor, up to $\pm$ 10 Nm. The estimated ankle torque derived from the deflection of the series springs (4) was then compared to the torque sensor reading. The root mean square error (RMSE) between the two signals was calculated to examine the effectiveness of torque estimation via the deflection of the series springs.

Next, a low-level torque control test was performed to validate the torque control accuracy and bandwidth. With the controller described in Section II.C, the simulator was commanded to track a chirp torque command whose frequency swept from 0-10 Hz and amplitude varying between 2-6 Nm. The RMSE between the torque command and the spring-deflection estimated torque was calculated.

The next test was to evaluate the performance of the high-level controller. Three different scenarios were tested: (1) no clonus (where the input was slow dorsiflexion), (2) unsustained clonus (fast dorsiflexion but not maintaining torque), and (3) sustained clonus (fast dorsiflexion and maintaining torque). The ankle angle reference trajectory was defined by the parameters in Table I (column labeled Original). Clinically, a response behavior will be considered to be "sustained clonus" when at least 5 consecutive beats are observed. The researcher (YP) manually performed the clonus assessment technique on the simulator, following guidance from an expert clinician (CMZ). All signals were sampled at 1 kHz and filtered using a 4th-order Butterworth filter with a cut-off frequency of 50 Hz.

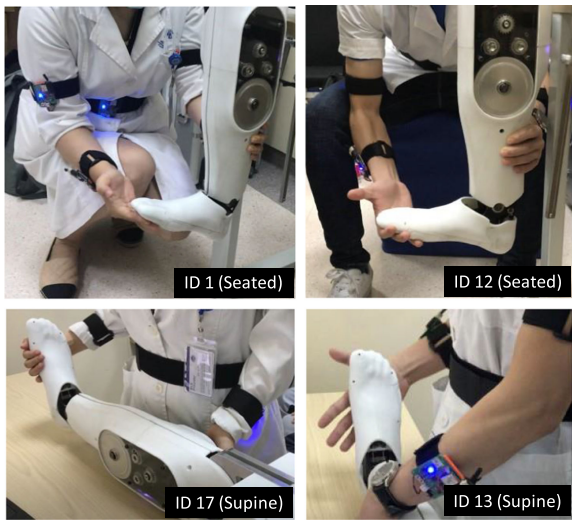

Fig. 4. Four subjects interacting with the simulator in two testing configurations that represented a patient in a seated or supine position.

E. Clinician Validation

To establish simulation realism, we coordinated an expert clinician validation study in the Rehabilitation Center at the Zhejiang Hospital in Hangzhou, China and invited physicians and physical therapists (PT) to examine how well the prototype simulator could simulate typical ankle clonus behavior. The inclusion criteria were that subjects should have at least of 2 years of clonus assessment experience and perform at least 10 assessments per month. All recruited subjects had no prior experience with interacting with a robotic training simulator. The study was approved by the IRB at the University of Illinois at Urbana-Champaign and Medical Ethics Committee of Zhejiang Hospital. The study was conducted over two consecutive days. Data analyses were based on input from 9 subjects on Day 1 and 8 on Day 2. The test protocol was the same for both days. Each subject was asked to induce sustained clonus at least three times in each of the two configurations (seated and supine), using the usual assessment technique (Fig. 4). For 16 out of 17 subjects, the first tested configuration was seated position. The controller parameters were the same between the two configurations. For each test configuration (i.e., seated and supine), the number of attempts to the first successful sustained clonus triggering was recorded. To document subjective feedback on the simulator performance and user experience, each subject answered a post-test questionnaire on 12 items. Only six simulation realism items were analyzed in this letter; the remaining six were regarding

TABLE II
SUMMARY OF QUESTIONNAIRE ITEMS FOR SIMULATION REALISM FEEDBACK

Item	Simulation Realism Item	Score				
		1	2	3	4	5
	Clonus Triggering Factors					
1	Dorsiflexion velocity threshold to trigger clonus	Too slow		About right		Too fast
	Clonus Maintaining Factors					
2	Sustaining torque threshold	Too Small		About Right		Too Large
	Clonus Simulation Characteristics					
3	Frequency of ankle oscillation	Too low		About right		Too high
4	Oscillation amplitude					
5	Resistance torque magnitude					
6	Mean oscillation position	Too DF				Too PF

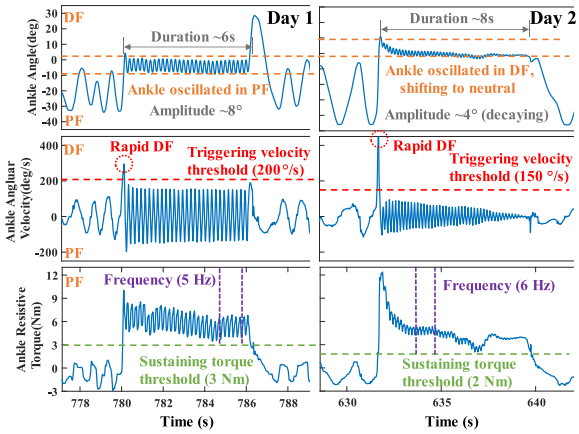

Fig. 5. Simulated clonus behavior before and after the controller revisions. (Left) Participant 8 on Day 1. (Right) Participant 17 on Day 2.

user experience and not presented here. Subjects were asked to evaluate these simulation items on a five-point scale, where a score of 3 matching the word "about right" was considered as an ideal score, meaning the simulated behavior felt similar to their clinical experience (Table II). To expedite controller design iteration, feedback received on Day 1 about the realism of the simulator was used to revise the clonus parameters, which were implemented in the simulator's controller during Day 2 testing (Table I, column Modified; Fig 5). Therefore, questionnaire scores between Day 1 and Day 2 were compared using two-sample, one-tailed t-tests with unequal variances ($\alpha = 0.05$) to study any significant change in simulation realism features per clinicians' feedback. In addition, all results were broken down into three subgroups based on job titles, i.e., all subjects, physicians only, PTs only.

III. RESULTS

A. Benchtop Evaluation Results

The custom SEA system's torque estimation and torque control capabilities were verified (Figs. 6 and 7). The torque estimated by the deflection of the series springs matched well with the torque sensor reading, where the average RMSE was 0.20 Nm (Fig. 6). The tuned controller was able to track a chirp torque signal up to 10 Hz without sign of motor saturation, with average RMSE <0.22 Nm (Fig. 7). Noticeable torque errors were found

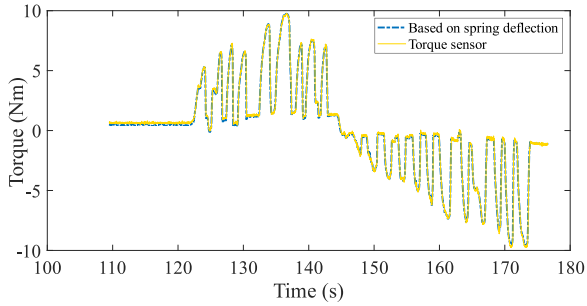

Fig. 6. Torque estimation test – comparison of torque computed from deflection of series springs and measured by a torque sensor.

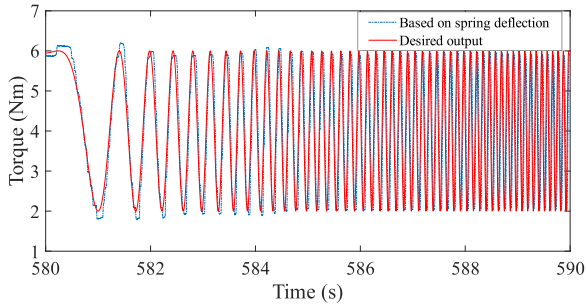

Fig. 7. Torque control accuracy and bandwidth test – comparison of torque computed from deflection of series springs and desired torque based on frequency swept from 0-10Hz and peak-peak amplitude of 4Nm.

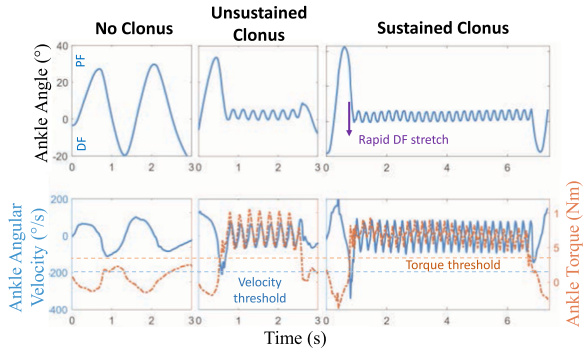

Fig. 8. Three operation states of the simulator: (Left) no clonus triggered due to low DF stretch speed. (Middle) Unsustained clonus triggered but not continued due to lack of DF torque. (Right) Sustained clonus behavior.

at the peaks of the sine wave at low frequency (i.e., ~1-3 Hz) and disappeared at higher frequency (i.e., > 3Hz). This error might be caused by motor gearbox stiction, since this error decreased as the frequency increased (i.e., motor started mainly experiencing dynamic friction). The high-level impedance controller was able to simulate the behavior of a patient with clonus and to switch between clonus and non-clonus modes based on velocity and torque thresholds (Fig. 8). Specifically, clonus could not be triggered under low dorsiflexion velocity (Fig. 8, Left) and was not sustained when applied torque on the foot dropped below the torque threshold (Fig. 8, Middle). Only a combination of rapid dorsiflexion (i.e., > 200 °/s) and applied torque on the foot (i.e., > 3 Nm) induced a sustained clonus behavior (Fig. 8, Right). The experimental ankle angle profile obtained during sustained

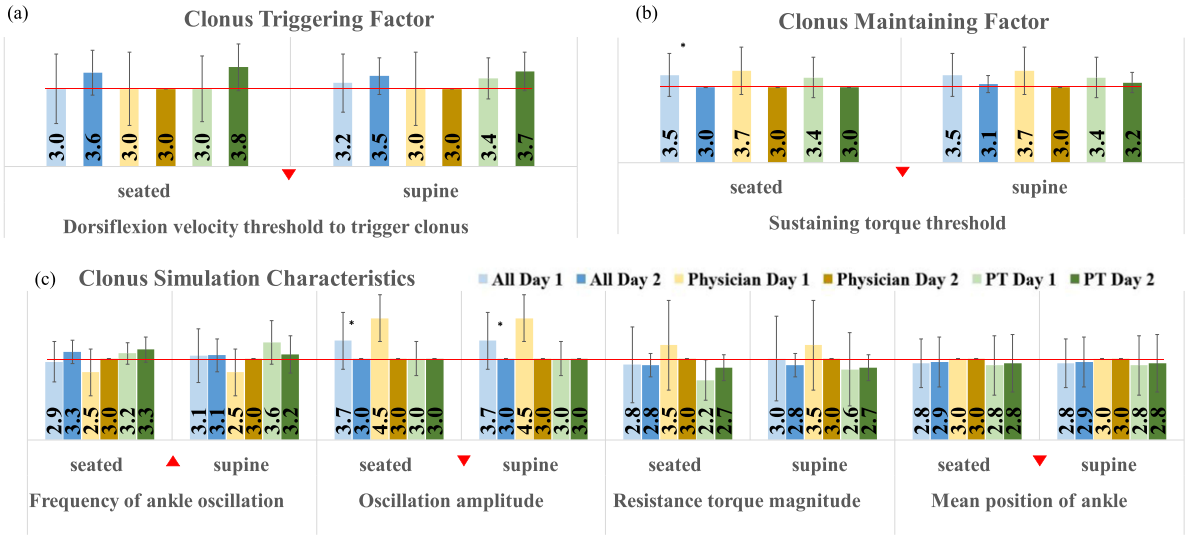

Fig. 9. Mean (standard deviation bars) of questionnaire scores for both days across three groups (i.e., all subjects, physicians only, and PTs only). Red lines indicate the ideal score. Red triangles indicate the tuned item and its tuning direction after Day 1 feedback (Table I). T-tests were only performed between All Day 1 and All Day 2 ($\alpha = 0.05$).

clonus case was qualitatively similar to a clinically-observed clonus behavior in terms of frequency and oscillation amplitude.

B. Clinician Validation Results

The simulator was validated by 17 clinicians in two configurations with the attempt numbers and questionnaire responses recorded. On average, all subjects could successfully trigger a sustained clonus response within 4-5 attempts in the first tested configuration and 2-3 in the second. The decrease in the number of attempts in the second configuration suggested a learning effect. For both days, regardless the controller tuning, physicians took noticeably fewer attempts to first success than PTs (i.e., average of 1.25 vs. 5.9 for the first tested configuration, and 1 vs. 2.8 for the second).

For each questionnaire item, the average score was calculated for each test day and by subgroup of physician or PT (Fig. 9). After the controller tuning/calibration, Day 2 subjects felt that simulated clonus behavior was generally "about right" in terms of realism and controller revision moved the mean scores of questionnaire items closer to the ideal with reduced scoring variance. Additionally, the average scores for sustaining torque threshold and oscillation amplitude were significantly reduced, moving closer to 3. There was little difference in scores between seated and supine configurations.

IV. Discussion

In this letter, a SEA-based ankle-foot simulator that replicated the behavior of a patient with ankle clonus and could be deployed in medical training programs as a robotic mock patient was proposed and developed. In the benchtop validations, the prototype simulator with the custom SEA system had very good estimated torque accuracy, torque control accuracy, and sufficient bandwidth for our application (i.e., 5-8 Hz of clonus oscillation) (Fig. 6 and 7). The use of a SEA resulted in a compact and cost-effective simulator design. The overall gear ratio of $\sim$60:1 in the prototype simulator allowed a commercial-grade, small motor (DJI M3508 motor size of 4.2cm in diameter and 6.6cm in length; cost of $140, including a C620 motor controller) to be used and all components fitted within the human lower-leg geometry. Thanks to the economical actuation system, this simulator with good torque control fidelity was developed in a total BOM cost less than $500. Just the force/torque sensor alone used in the previous designs cost more than the overall cost of our device. Therefore, the SEA design not only demonstrated good torque control capability but also lowered the cost barrier for the training simulator to be adopted.

To validate the realism of clonus simulation, 17 clinicians with experience doing clonus assessment evaluated the clinical performance of the prototype simulator. Feedback from the Day 1 session with 9 clinicians was used to refine the controller behavior and then the modified controller was evaluated during the Day 2 session with 8 different clinicians (Table I, Fig. 5). After revising the clonus controller parameters prior to the Day 2 session, the variance of scores decreased in all items except for mean ankle position, which stayed the same. Note that the large score variances on Day 1 (Fig. 9) may be partly due to the large variance in years of experience among Day 1 subjects (SD: 5.3 on Day 1 vs. SD: 2.7 on Day 2). Subjects on average demonstrated quick adaptation to the simulated clonus behavior and successfully triggered a sustain clonus on the simulator within a few trials using their usual technique. The small number of attempts to success implied that the simulator's control logic (i.e., triggering and maintaining clonus) aligned with participants' existing clinical knowledge and training. Physicians were found to be able to successfully trigger sustained clonus with fewer attempts than PTs. It is possible that this difference was due to physical therapists' job habit/mindset to suppress clonus in patients, rather than to induce and assess clonus like physicians. This additional adaptation for PTs might have caused them to take longer to succeed.

Valuable feedback was received throughout the clinician validation study and several design limitations were recognized. Subjects commented that in the supine configuration, the patient's leg will often be externally rotated at the hip with the

knee flexed; however, our prototype lacked a thigh and hip joint. Furthermore, some level of randomized variation was suggested in the controller parameters to prepare the trainees with the unpredictable nature of clinical cases. Similarly, simulations of other common abnormal muscle behaviors at the ankle joint such as rigidity and spasticity (as selected) were suggested to increase training sophistication. Therefore, future work should involve enhancing the dexterity of the simulator to match the DOFs of the lower limb; and in order to maximize the potential of device hardware, more variations of simulation algorithm should be implemented.

V. Conclusion

The prototype ankle-foot SEA-based simulator was validated in both benchtop tests and clinician evaluation. The experimental results and clinical feedback were promising and suggested that this device could mimic a real patient by (1) generating a simulated clonus behavior whose triggering and maintaining mechanism aligned with clinicians' experience, and (2) recreating a relatively realistic haptic response of affected muscles. However, the device still lacks the full dexterity of a human lower-extremity, which requires further design iterations. The use of a SEA system resulted in not only a high-performance research simulator, but also a cost-effective and compact design that could become viable to be widely deployed as a valuable training tool for learners.

Acknowledgment

We thank the clinician subjects, Ben Yang, Zeying Lang, Dmitry Ilchenko, Prateek Garag, and graduate students in Prof. Liu's and Prof. Yang's labs for their support.

References

[1] S. Y. Song, C. M. Zallek, and E. T. Hsiao-Wecksler, "Quantification of spasticity in upper-arm muscles using the PVRM (Position, velocity, and resistance meter)," in *Proc. Des. Med. Devices Conf.*, 2019.

[2] A. A. Mullick, N. K. Musampa, A. G. Feldman, and M. F. Levin, "Stretch reflex spatial threshold measure discriminates between spasticity and rigidity," *Clin. Neurophysiol.*, vol. 124, no. 4, pp. 740–751, 2013.

[3] A. Pandyan, "A Review of the Properties and Limitations of the Ashworth and Midified Ashworth Scales as Measures of Spasticity," *Clin. Rehabil.*, vol. 13, pp. 373–383, 1999.

[4] F. Biering-Sørensen, J. B. Nielsen, and K. Klinge, "Spasticity-Assessment: A Review," *Spinal Cord*, vol. 44, no. 12, pp. 708–722, 2006.

[5] S. C. Allison, L. D. Abraham, and C. L. Petersen, "Reliability of the Modified Ashworth Scale in the Assessment of Plantarflexor Muscle Spasticity in Patients with Traumatic Brain Injury," *Int. J. Rehabil. Res.*, vol. 19, no. 1, pp. 67–78, 1996.

[6] M. Blackburn, P. van Vliet, and S. Mockett, "Reliability of Measurements Obtained With the Modified Ashworth Scale in the Lower Extremities of People With Stroke," *Phys Ther*, vol. 82, no. 1, pp. 25–34, 2002.

[7] Y. Takhashi *et al.*, "Development of an Upper Limb Patient Simulator for Physical Therapy Exercise," in *Proc. IEEE Int. Conf. Rehabil. Robot.*, 2011, pp. 1–4.

[8] K. Kunkler, "The Role of Medical Simulation: An Overview," *Int. J. Med. Robot. Comput. Assist. Surg.*, vol. 2, pp. 203–2210, 2006.

[9] H. S. Park, J. Kim, and D. L. Damiano, "Development of a Haptic Elbow Spasticity Simulator (HESS) for Improving Accuracy and Reliability of Clinical Assessment of Spasticity," *IEEE Trans. Neural Syst. Rehabil. Eng.*, vol. 20, no. 3, pp. 361–370, 2012.

[10] D. I. Grow *et al.*, "Haptic Simulation of Elbow Joint Spasticity," in *Proc. Symp. Haptics Interfaces for Virtual Environ. Teleoperator Syst. 2008 - Proc., Haptics*, pp. 475–476.

[11] C. Wang *et al.*, "Development of an Arm Robot for Neurologic Examination Training," in *Proc. IEEE Int. Conf. Intell. Robots Syst.*, 2012, pp. 1090–1095.

[12] S. Ishikawa *et al.*, "Assessment of Robotic Patient Simulators for Training in Manual Physical Therapy Examination Techniques," *PLoS One*, vol. 10, no. 4, 2015, Art. no. e0126392.

[13] J. Liang, Y. Pei, R. H. Ewoldt, S. R. Tippett, and E. T. Hsiao-Wecksler, "Passive Hydraulic Training Simulator for Upper Arm Spasticity," *J. Mech. Robot.*, vol. 12, no. 4, 2020, Art. no. 045001.

[14] T. Kikuchi, K. Oda, and J. Furusho, "Leg-Robot for Demonstration of Spastic Movements of Brain-Injured Patients with Compact Magnetorheological Fluid Clutch," *Adv. Robot.*, vol. 24, no. 5–6, pp. 671–686, 2010.

[15] H. Okumura *et al.*, "Exoskeleton Simulator of Impaired Ankle: Simulation of Spasticity and Clonus," in *Haptic Interaction*, Tokyo, Springer, 2015, pp. 209–214.

[16] T. R. Coles, D. Meglan, and N. W. John, "The Role of Haptics in Medical Training Simulators: A Survey of the State of the Art," *IEEE Trans. Haptics*, vol. 4, no. 1, pp. 51–66, Jan./Mar. 2011.

[17] P. A. LeWitt, "Clonus," *Encycl. Neurol. Sci.*, vol. 1, no. 1976, pp. 806–806, 2014.

[18] G. L. Gottlieb and G. C. Agarwal, "Physiological Clonus in Man," *Exp. Neurol.*, vol. 54, no. 3, pp. 616–621, 1977.

[19] A. Rossi, R. Mazzocchio, and C. Scarpini, "Clonus in Man: A Rhythmic Oscillation Maintained by a Reflex Mechanism," *Electroencephalogr. Clin. Neurophysiol.*, vol. 75, no. 1–2, pp. 56–63, 1990.

[20] I. Boyraz, H. Uysal, B. Koc, and H. Sarman, "Clonus: Definition, Mechanism, Treatment," *Med. Glas.*, vol. 12, no. 1, pp. 19–26, 2015.

[21] J. M. Hidler and W. Z. Rymer, "A Simulation Study of Reflex Instability in Spasticity: Origins of Clonus," *IEEE Trans. Rehabil. Eng.*, vol. 7, no. 3, pp. 327–340, 1999.

[22] E. G. Walsh and G. W. Wright, "Patellar Clonus: An Autonomous Central Generator," *J. Neurol. Neurosurg. Psychiatry*, vol. 50, no. 9, pp. 1225–1227, 1987.

[23] K. J. Manella, K. E. Roach, and E. C. Field-Fote, "Temporal Indices of Ankle Clonus and Relationship to Electrophysiologic and Clinical Measures in Persons with Spinal Cord Injury," *J. Neurol. Phys. Ther.*, vol. 41, no. 4, pp. 229–238, 2017.

[24] J. A. Beres-Jones, T. D. Johnson, and S. J. Harkema, "Clonus after Human Spinal Cord Injury Cannot Be Attributed Solely to Recurrent Muscle-Tendon Stretch," *Exp Brain Res*, vol. 149, pp. 222–236, 2003.

[25] J. E. Butler, S. Godfrey, and C. K. Thomas, "Depression of Involuntary Activity in Muscle Paralyzed by Spinal Cord Injury," *Muscle Nerve*, vol. 33, no. 5, pp. 637–644, 2006.

[26] M. R. Dimitrijevic, P. W. Nathan, and A. M. Sherwood, "Clonus: The Role of Central Mechanisms," *J. Neurol. Neurosurg. Psychiatry*, vol. 43, no. 4, pp. 321–332, 1980.

[27] D. M. Wallace, B. H. Ross, and C. K. Thomas, "Motor Unit Behavior during Clonus," *J. Appl. Physiol.*, vol. 99, no. 6, pp. 2166–2172, 2005.

[28] W. W. Campbell and R. N. DeJong, *DeJong's the Neurologic Examination*, Lippincott Williams & Wilkins, 2005.

[29] E. De Vlugt *et al.*, "Clonus Is Explained from Increased Reflex Gain and Enlarged Tissue Viscoelasticity," *J. Biomech.*, vol. 45, no. 1, pp. 148–155, 2012.

[30] E. De Vlugt *et al.*, "The Relation between neuromechanical parameters and ashworth score in stroke patients," *J. Neuroeng. Rehabil.*, vol. 7, no. 1, pp. 5–7, 2010.

[31] N. Paine *et al.*, "Actuator Control for the NASA-JSC Valkyrie Humanoid Robot: A Decoupled Dynamics Approach for Torque Control of Series Elastic Robots," *J. F. Robot.*, vol. 32, no. 3, pp. 378–396, 2015.

[32] M. Hutter *et al.*, "ANYmal - A highly mobile and dynamic quadrupedal robot," in *Proc. IEEE/RSJ Int. Conf. Intell. Robots Syst.*, 2016, pp. 38–44.

[33] E. J. Rouse, L. M. Mooney, and H. M. Herr, , "Clutchable Series-Elastic Actuator: Implications for Prosthetic Knee Design," *Int. J. Rob. Res.*, vol. 33, no. 13, pp. 1611–1625, 2014.

[34] P. De Leva, "Adjustments to Zatsiorsky-Seluyanov's Segment Inertia Parameters," *J. Biomech.*, vol. 29, no. 9, pp. 1223–1230, 1996.

[35] J. Pratt, B. Krupp, and C. Morse, "Series Elastic Actuators for High Fidelity Force Control," *Ind. Robot An Int. J.*, vol. 29, no. 3, pp. 234–241, 2002.

[36] P. Garag, "Mechatronic and biomechanical considerations toward the design of an ankle clonus simulator," M.S. thesis, Dept. Mech. Sci. Engr., Univ. of Illinois at Urbana-Champaign, IL, USA, 2019.

[37] J. W. Sensinger and R. F. Weir, "Improvements to series elastic actuators," in *Proc. 2nd IEEE/ASME Int. Conf. Mechatronic Embedded Syst. Appl.*, pp. 1–7, 2006.